Point Set Registration based on Multi-Object Metrics

1st Pablo Barrios
Dept. Electrical Engineering
Universidad de Chile
Santiago, Chile
pbarrios@ing.uchile.cl

2nd Martin Adams, *IEEE Senior Member*
Dept. Electrical Engineering &
Advanced Mining Technology Center (AMTC)
Universidad de Chile
Santiago, Chile
martin@ing.uchile.cl

***Abstract*—In robotics and computer vision, point set registration is necessary in many tasks, for example in estimating the motion of a sensor/sensors between subsequent scans containing point/feature sets. Currently, the Iterated Closest Point (ICP) method and its variants have been presented as possible solutions to this problem. However most of these methods lack robustness when random spatial and detection errors are present. This is because ICP methods typically use an L2 metric as part of their optimization criteria, which is unable to penalize cardinality errors. Therefore, this article presents a registration technique based on the multi-object Optimal Sub-Pattern Assignment (OSPA) and Cardinalized Optimal Linear Assignment (COLA) metrics, which penalize data differences based on both cardinality and spatial errors. This allows scan registration to take place in the presence of both inter-scan translation and orientation as well as detection errors.**

***Index Terms*—Point Set Registration, Scan Matching, Multi-Object Metrics.**

I. Introduction

In [1],[2], the multi-object metrics OSPA and COLA were proposed as solutions to the evaluation of error between two different sets of points $\mathcal{M}$ and $\widehat{\mathcal{M}}$. These multi-object metrics have applications in assessing multi-target tracking and robotic mapping algorithms in the presence of both state and state cardinality errors. This article presents an extension of these multi-object metrics, which estimates the transformation between coordinate systems containing two point sets. This concept is useful for estimating the motion of a sensor/sensors between subsequent scans containing point/feature sets. An advantage of this extension is that these metrics take into account cardinality and spatial errors between point/feature sets, in a joint manner. This allows scan registration to take place in the presence of both inter-scan translation and orientation as well as detection errors.

II. The Registration Optimization Problem

To define the optimization problem, it is necessary to consider two sets: The *reference* set as $\mathcal{M} = \{\mathbf{m}^1, \ldots, \mathbf{m}^{\mathrm{m}}\}$ and its *model* set $\widehat{\mathcal{M}}' = \{\widehat{\mathbf{m}}^1, \ldots, \widehat{\mathbf{m}}^{\widehat{\mathrm{m}}}\}$ recorded in different frames of reference defined by $\mathbf{S}$ and $\mathbf{S}'$ respectively. Our goal is to find a solution of:

$$d^{(c,p)}(\mathcal{M}, \widehat{\mathcal{M}}') = \min_{\mathbf{R}(\theta),\mathbf{t}} d^{(c,p)}(\mathcal{M}, \widehat{\mathcal{M}}(\mathbf{R}(\theta), \mathbf{t})) \tag{1}$$

where $d^{(c,p)}(\mathcal{M}, \widehat{\mathcal{M}}')$ is given by either the OSPA or COLA metrics, $\widehat{\mathcal{M}}(\mathbf{R}(\theta), \mathbf{t})$ is the transformed set of $\widehat{\mathcal{M}}'$ into the frame of reference $\mathbf{S}$ via rotation matrix $\mathbf{R}(\theta)$ and translation vector $\mathbf{t}$, c is the chosen metric's cut-off distance and p the power used in the metric [2]. Without loss of generality, this article considers 2D space in which

$$\widehat{\mathcal{M}}(\mathbf{R}(\theta), \mathbf{t}) = \{\mathbf{R}(\theta)\widehat{\mathbf{m}}^1 + \mathbf{t}, \ldots, \mathbf{R}(\theta)\widehat{\mathbf{m}}^{\widehat{\mathrm{m}}} + \mathbf{t}\} \tag{2}$$

$$\mathbf{R}(\theta) = \begin{bmatrix} \cos\theta & -\sin\theta \\ \sin\theta & \cos\theta \end{bmatrix} \tag{3}$$

$$\mathbf{t} = \begin{bmatrix} t_x \\ t_y \end{bmatrix} \tag{4}$$

$$\theta \in [-\pi, \pi] \tag{5}$$

where t_x and t_y are the x and y components of the translation vector.

III. Solving the Registration Optimization Problem

In general, solving (1) is complex, because the function:

$$f^{(c,p)}(\theta, \mathbf{t}) = d^{(c,p)}(\mathcal{M}, \widehat{\mathcal{M}}(\mathbf{R}(\theta), \mathbf{t})) \tag{6}$$

belongs to a family of non-convex functions, with several local maxima and minima, which depend on both c and p. Therefore, a requirement for the solution of this problem is a method which calculates the best solution in a global sense. In the literature, there exist many methods related to global optimization in the context of point set registration. Recently, the state of the art Globally Optimal ICP (Go-ICP) algorithm was presented [3]. This iterative algorithm uses a combination of two methods. Initially, it performs the classical ICP algorithm in order to find a local minima. Then, it performs a Branch and Bound (B&B) global optimization to explore within the limits of the parameters θ (equation (5)) and $\mathbf{t}$. This is carried out in order to update the upper bounds of the objective function during the search process. In other words, if possible, the B&B algorithm is able to force the objective function to decrease after an ICP iteration (see Fig. 1). A disadvantage of the Go-ICP algorithm is its L2 objective cost function. Before this cost function can be used, Go-ICP requires trimming strategies to remove outliers. These factors are based on heuristics. Another problem with this algorithm is the computational complexity of the B&B approach, which increases exponentially with the chosen resolution of variables θ and $\mathbf{t}$ [4]. Other alternatives to solve this global optimization

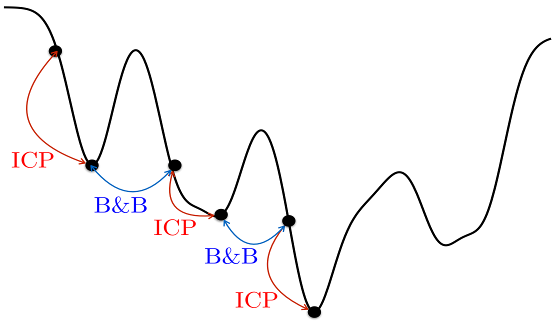

Fig. 1: The concept of Go-ICP presented as a collaborative method between the ICP and B&B methods.

problem, in the context of point set registration, are stochastic optimization such as Genetic Algorithms [5], Particle Swarm Optimization (PSO) [6], Particle Filtering [7] and Simulated Annealing [8].

Particle Swarm Optimization (PSO) is currently applied in several disciplines due to its robustness in finding global optimal solutions in few steps with a set of particles exploring an objective function. These methods are based on interactive particles $\mathbf{p}^i(k)$, in that all members of the particle population communicate their cost function values $g(\mathbf{x}^i(k))$ to the other particles $\mathbf{p}^j(k)$, $j \neq i$. Denote the set of particles at time k as $\mathcal{P}(k) = \{\mathbf{p}^1(k), \ldots, \mathbf{p}^{|\mathcal{P}|}(k)\}$. $\mathbf{p}^i(k) = [\mathbf{x}^i(k), \mathbf{x}^i_{\text{local}}(k), \mathbf{v}^i(k), g(\mathbf{x}^i(k))]^\top$ represents the particle i at time k. Its position is $\mathbf{x}^i(k)$, with best personal experienced position $\mathbf{x}^i_{\text{local}}(k)$, velocity $\mathbf{v}^i(k)$ and fitness cost value $g(\mathbf{x}^i(k))$, where in this case the function $g()$ will be the cost function defined in equation (6). $\mathbf{x}^i_{\text{local}}(k)$ is defined as the position at which particle i reached its minimum (maximum) cost value throughout its entire motion history. Ultimately, the algorithm moves the particles towards the best global position $\mathbf{x}_{\text{global}}(k)$ which satisfies $g(\mathbf{x}_{\text{global}}(k)) < g(\mathbf{x}^i(k))$ for minimization or $g(\mathbf{x}_{\text{global}}(k)) > g(\mathbf{x}^i(k))$ for maximization, for all i and k.

IV. Registration in the Context of Multi-Object Metrics

Conceptually, point set registration requires the correct computation of point/feature relative translation, rotation and inter scan detection errors. For this reason we define the population state of each particle as follows:

$$\mathbf{p}^i(k) = \begin{bmatrix} \mathbf{x}^i(k) \\ \mathbf{x}^i_{\text{local}}(k) \\ \mathbf{v}^i(k) \\ g(\mathbf{x}^i(k)) \end{bmatrix}, \mathbf{x}^i(k) = \begin{bmatrix} \theta^i(k) \\ t_x{}^i(k) \\ t_y{}^i(k) \end{bmatrix} \quad (7)$$

$$\mathbf{x}^i_{\text{local}}(k) = \begin{bmatrix} \theta^i_{\text{local}}(k) \\ t^i_{x,\text{local}}(k) \\ t^i_{y,\text{local}}(k) \end{bmatrix}, \mathbf{v}^i(k) = \begin{bmatrix} v^i_\theta(k) \\ v_{t_x}{}^i(k) \\ v_{t_y}{}^i(k) \end{bmatrix} \quad (8)$$

$$g(\mathbf{x}^i(k)) = f^{(c,p)}(\mathbf{x}^i(k)^\top) \quad (9)$$

where its objective function $f^{(c,p)}(\mathbf{x}^i(k)^\top)$ is given by equation (6). To initialize the PSO algorithm [9], the concept adopted is to spread N particles randomly from rest, i.e. $\mathbf{v}^i(k=0) = 0$, with positions $\mathbf{x}^i(k=0)$ uniformly distributed in the domain of the objective function to minimize. Finally, the method considers an iterative motion model of the particles given by the following equations:

$$\begin{aligned} \mathbf{v}^i(k+1) &= \chi \mathbf{v}^i(k) + c_1 r_1 (\mathbf{x}^i_{\text{local}}(k) - \mathbf{x}^i(k)) \quad (10) \\ &+ c_2 r_2 (\mathbf{x}_{\text{global}}(k) - \mathbf{x}^i(k)) \\ \mathbf{x}^i(k+1) &= \mathbf{x}^i(k) + \mathbf{v}^i(k+1). \quad (11) \end{aligned}$$

where r_1, r_2 are random numbers between 0 and 1, $0 < \chi \leq 1$ is the damping coefficient, and c_1 and c_2 are the local and social accelerations. There are then two possibilities: First, if $\mathbf{x}^i_{\text{local}}(k) \neq \mathbf{x}_{\text{global}}(k)$, the particle i will remain in random motion in order to find a global minima. Otherwise, if $\mathbf{x}^i_{\text{local}}(k) = \mathbf{x}_{\text{global}}(k)$, particle i will execute an orbit attracted to the global minima, and the particle's velocity decreases its value for every iteration due to the damping coefficient χ.

V. Results

The following section presents the registration performance of the PSO-OSPA, PSO-COLA and Go-ICP algorithms in cases when either spatial noise or cardinality errors or both are included. To execute the PSO-COLA and PSO-OSPA algorithms, 100 iterations will be performed with $N = 50$ particles uniformly distributed with the OSPA/COLA metric cut-off parameter $c = 0.025$[m] and power $p = 2$. The PSO damping and acceleration coefficients, $\chi = 0.7298$ and $c_1 = c_2 = 2.05$ are chosen according to [9]. To execute Go-ICP a threshold value for the MSE ϵ, and trimming factor are required. As suggested in [3], these were set to $\epsilon = 0.001$, and trimming factor 10%. For testing purposes, the Chui & Rangarajan datasets are used [10]. Classically these datasets have been applied for benchmarking solutions in the context of non-rigid point set registration algorithms. Due to the shape symmetries of the datasets, the solutions of rigid registration are difficult to solve. Finally, to evaluate the registration performance, the multi-object OSPA and COLA metrics will be used.

A. Creating the Reference and Model Datasets

In order to create a reference and model data set $\mathcal{M}$ and $\widehat{\mathcal{M}}$ respectively for rigid registration, from a single data set $\mathcal{D}$, the following construction steps are used:

(1) Initially it is necessary to duplicate the dataset $\mathcal{D}$ as $\mathcal{M}_o$ and $\widehat{\mathcal{M}}_o$, where $\mathcal{M}_o = \widehat{\mathcal{M}}_o = \mathcal{D}$, $\mathcal{M}_o$ is the *initial reference* set and $\widehat{\mathcal{M}}_o$ is the *initial model* set.
(2) Create a new *reference* set $\mathcal{M} \subset \mathcal{M}_o$, in order to simulate missed detections (MD).
(3) Create a new subset $\widehat{\mathcal{M}}_s \subset \widehat{\mathcal{M}}_o$, in order to simulate false alarms (FA) with respect to $\mathcal{M}$.
(4) For each point in $\widehat{\mathcal{M}}_s$ random vectors $\mathbf{v}^i$, are added to each point's coordinates to generate a set $\widehat{\mathcal{M}}_e$ with spatial errors between corresponding points, i.e. $\widehat{\mathcal{M}}_e = \{\mathbf{m}^i +$

$\mathbf{v}^i\}_{i=1}^{|\mathcal{M}_s|}$. The vectors $\mathbf{v}^i$ are normally distributed with zero mean and standard deviation σ.

(5) Define the set of outliers $\widehat{\mathcal{D}}_e$. Then the set $\widehat{\mathcal{M}}_e$ with detection errors will be defined as $\widehat{\mathcal{M}}_f = \widehat{\mathcal{M}}_e \cup \widehat{\mathcal{D}}_e$.

(6) Define the *model* set $\widehat{\mathcal{M}}$ as the transform of the set $\widehat{\mathcal{M}}_f$ with rotation $\mathbf{R}(\theta)$ and translation $\mathbf{t}$ given by $\widehat{\mathcal{M}} = \{\mathbf{R}(\theta)\widehat{\mathbf{m}}_f^i + \mathbf{t}\}_{i=1}^{|\mathcal{M}_f|}$

The deterministic transformations to be used will be $[\theta^F, t_x^F, t_y^F] = [180^o, -0.5[m], 1[m]]$ and $[\theta^C, t_x^C, t_y^C] = [37^o, -0.26[m], 0.38[m]]$ for the Chui & Rangarajan fish and Chinese character datasets respectively [10]. These transformations are shown in Fig. 2. In the case of spatial noise,

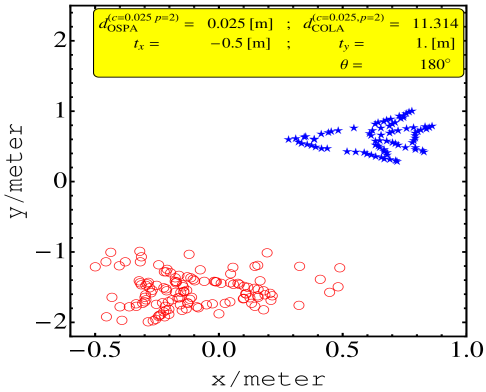

(a) *Fish dataset.*

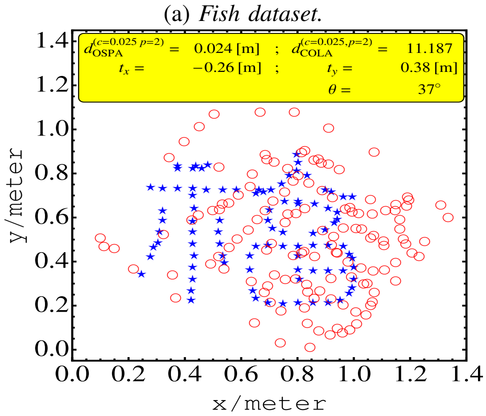

(b) *Chinese character dataset.*

Fig. 2: *The original (blue stars) and transformed and corrupted (red circles) Chui & Rangarajan fish and Chinese character datasets with transforms given in each graph.*

the concept is to determine how the registration process is affected when random vectors $\mathbf{v}^i$ distort the model set. Consequently, the corresponding analysis will consider the registration performance while varying the standard deviation σ. In this case, the cardinality error between the reference and the model set remains constant for each scenario.

In the case of cardinality errors, it will be determined how the registration process is affected when random outliers are successively added to the model set. In this case, the spatial errors between the reference and model sets are implemented with random vectors $\mathbf{v}^i$ with constant standard deviation σ.

B. Registration performance

This section will highlight the differences between the PSO-OSPA, PSO-COLA and Go-ICP algorithms for different levels of random noise.

1) Spatial noise: The addition of low spatial noise is shown in Figs. 5a and 5c for the the fish and Chinese character respectively. In each graph the estimated translation $\widehat{t}_x$, $\widehat{t}_y$ and rotation $\widehat{\theta}$, are given for each algorithm. Under these circumstances the PSO-COLA, PSO-OSPA and Go-ICP algorithms achieve similar registration performance. In each case they are close to their true values. Each graph also shows the OSPA and COLA metric values calculated from the differences between the reference set $\mathcal{M}$ and the model set $\widehat{\mathcal{M}}$ after execution of each algorithm. Increasing the spatial noise, results in Figs. 5b and 5d. In this case Go-ICP is unable to achieve the registration performance of PSO-COLA and PSO-OSPA as reflected in the estimated translation and rotation variables $\widehat{t}_x$, $\widehat{t}_y$ and $\widehat{\theta}$. This is confirmed by the OSPA and COLA metrics in figure Fig 5b and by the COLA metric only in Fig 5d, when expressing the OSPA metric values to three significant figures.

Fig. 3 shows the OSPA metric values corresponding to the performances of each algorithm for multiple values of the spatial standard deviation σ. Again it can be seen that as σ is increased, the PSO-OSPA and PSO-COLA algorithms perform similarly, while outperforming the Go-ICP algorithm.

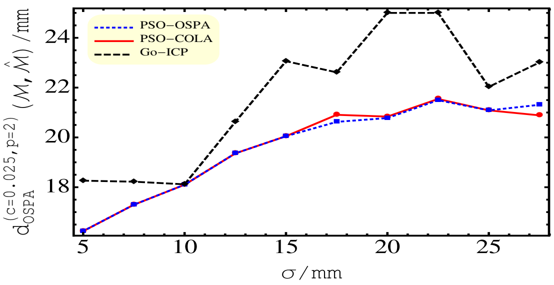

(a) *Fish*

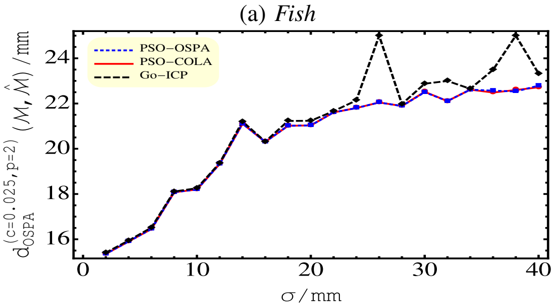

(b) *Chinese character*

Fig. 3: *Registration performance based on the OSPA metric when the spatial noise standard deviation σ is varied. The OSPA metric cut-off parameter $c = 0.025$ and power $p = 2$.*

2) Cardinality errors: Figs. 6a and 6c show the registration results when there are no cardinality errors between the reference and model datasets $\mathcal{M}$ and $\widehat{\mathcal{M}}$. In each case, a spatial noise standard deviation of constant value $\sigma = 20$[mm] was used. As can be seen, the registration performances are similar in each case, with a slight decrease in the performance of the

Go-ICP algorithm, as reflected by each graph's OSPA and COLA metric values.

Figs. 6b and 6d show the registration results for each algorithm, when a higher number of detection errors is introduced into each model set $\widehat{\mathcal{M}}$. In this case, Go-ICP yields poor results, due to its sensitivity to the heuristic choice of the trimming factor. In contrast, the PSO-OSPA and PSO-COLA algorithms yield superior results because of their automatic penalization of cardinality errors, circumventing the necessity of outlier rejection heuristics.

Fig. 4 shows the registration algorithms' performances for multiple cardinality error values. It can be seen that under increasing cardinality error, the PSO-OSPA and PSO-COLA algorithms demonstrate equivalent registration performances, which are both superior to that of the Go-ICP algorithm.

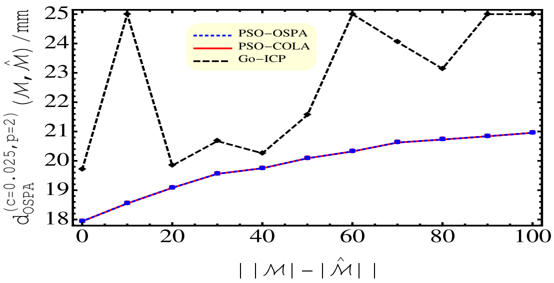

(a) *Fish*

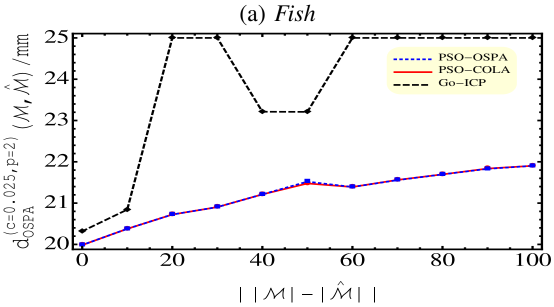

(b) *Chinese Character*

Fig. 4: *Registration performance based on the OSPA metric when the cardinality error* $||\mathcal{M}|-|\widehat{\mathcal{M}}||$ *is varied. The OSPA metric cut-off parameter* $c = 0.025$ *and power* $p = 2$.

3) Computational Complexity: The PSO-COLA and PSO-OSPA registration algorithms both have a computational complexity $\mathcal{O}(N \times I \times \max(|\mathcal{M}|, |\widehat{\mathcal{M}}|)^3 + N \times d)$, where N is the number of particles, I is the number of iterations and d is the number of parameters, which in this case is $d = 3$ (θ, t_x, t_y).

The computational complexity of the Go-ICP algorithm is dependent on the B&B approach. It increases exponentially with the chosen resolution of variables θ and $\mathbf{t}$ [4].

VI. Summary

This article presents the application of the multi-object OSPA and COLA metrics for point set registration. The algorithms presented, used PSO to find an estimate of the rigid transformations $\mathbf{R}(\theta)$ and $\mathbf{t}$ between reference and model sets, where the cost function was either the OSPA or COLA metric. To test the registration performance, the Chui & Rangarajan datasets were used. For comparisons, the state of the art Go-ICP registration algorithm was used as a benchmark. The results show improvements over Go-ICP in accuracy and robustness in cases when either spatial and/or cardinality errors exist. This is due to the ability of the OSPA and COLA metrics to reflect cardinality errors in their cost values.

Acknowledgements

The authors acknowledge "Becas Conicyt - Doctorado Nacional, 2012". Conicyt-Fondecyt project 1150930 and the Advanced Mining Technology Center (AMTC).

References

[1] D. Schuhmacher, B. Vo, and B. Vo, "A consistent metric for performance evaluation of multi-object filters," *IEEE Transactions on Signal Processing*, vol. 86, no. 8, pp. 3447–3457, 2008.

[2] P. Barrios, M. Adams, K. Leung, F. Inostroza, G. Naqvi, and M. E. Orchard, "Metrics for evaluating feature-based mapping performance," *IEEE Transactions on Robotics*, vol. 33, no. 1, pp. 198–213, 2017.

[3] J. Yang, H. Li, D. Campbell, and Y. Jia, "Go-icp: a globally optimal solution to 3d icp point-set registration," *IEEE transactions on pattern analysis and machine intelligence*, vol. 38, no. 11, pp. 2241–2254, 2016.

[4] J. Straub, T. Campbell, J. P. How, and J. W. Fisher, III, "Efficient global point cloud alignment using bayesian nonparametric mixtures," in *The IEEE Conference on Computer Vision and Pattern Recognition (CVPR)*, July 2017, pp. 2941–2950.

[5] L. Silva, O. R. P. Bellon, and K. L. Boyer, "Precision range image registration using a robust surface interpenetration measure and enhanced genetic algorithms," *IEEE transactions on pattern analysis and machine intelligence*, vol. 27, no. 5, pp. 762–776, 2005.

[6] M. P. Wachowiak, R. Smolíková, Y. Zheng, J. M. Zurada, and A. S. Elmaghraby, "An approach to multimodal biomedical image registration utilizing particle swarm optimization," *IEEE Transactions on evolutionary computation*, vol. 8, no. 3, pp. 289–301, 2004.

[7] R. Sandhu, S. Dambreville, and A. Tannenbaum, "Point set registration via particle filtering and stochastic dynamics," *IEEE transactions on pattern analysis and machine intelligence*, vol. 32, no. 8, pp. 1459–1473, 2010.

[8] C. Papazov and D. Burschka, "Stochastic global optimization for robust point set registration," *Computer Vision and Image Understanding*, vol. 115, no. 12, pp. 1598–1609, 2011.

[9] M. Clerc and J. Kennedy, "The particle swarm-explosion, stability, and convergence in a multidimensional complex space," *IEEE transactions on Evolutionary Computation*, vol. 6, no. 1, pp. 58–73, 2002.

[10] H. Chui and A. Rangarajan, "A new point matching algorithm for non-rigid registration," *Computer Vision and Image Understanding*, vol. 89, no. 2, pp. 114–141, 2003.

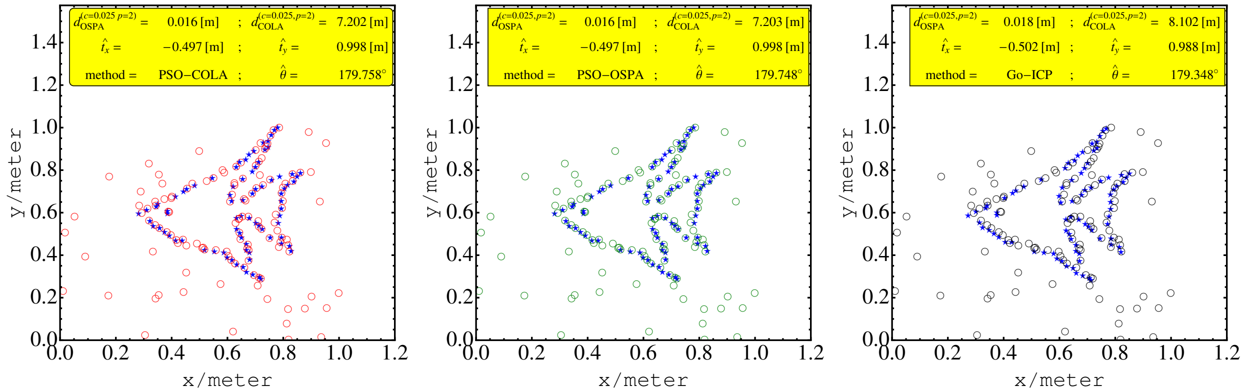

(a) *Registration results with $\sigma = 5$[mm].*

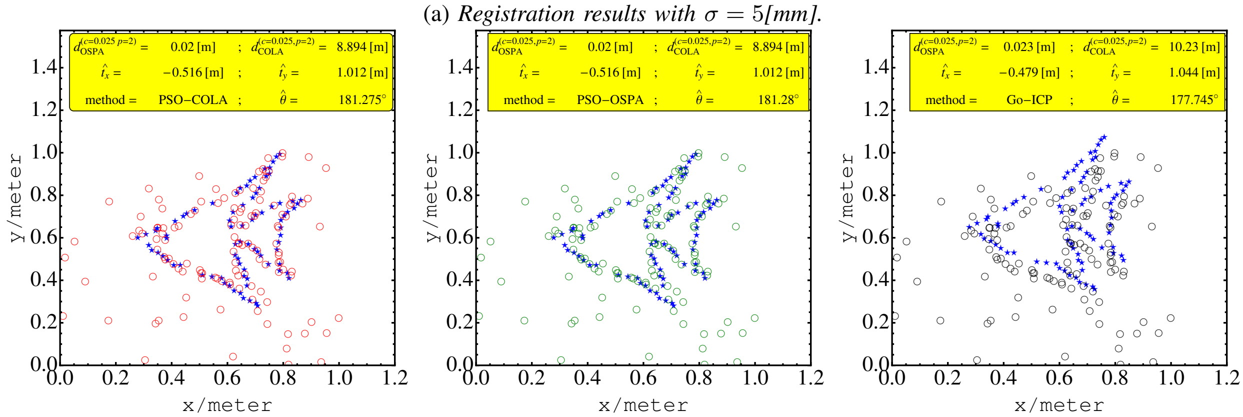

(b) *Registration results with $\sigma = 15$[mm].*

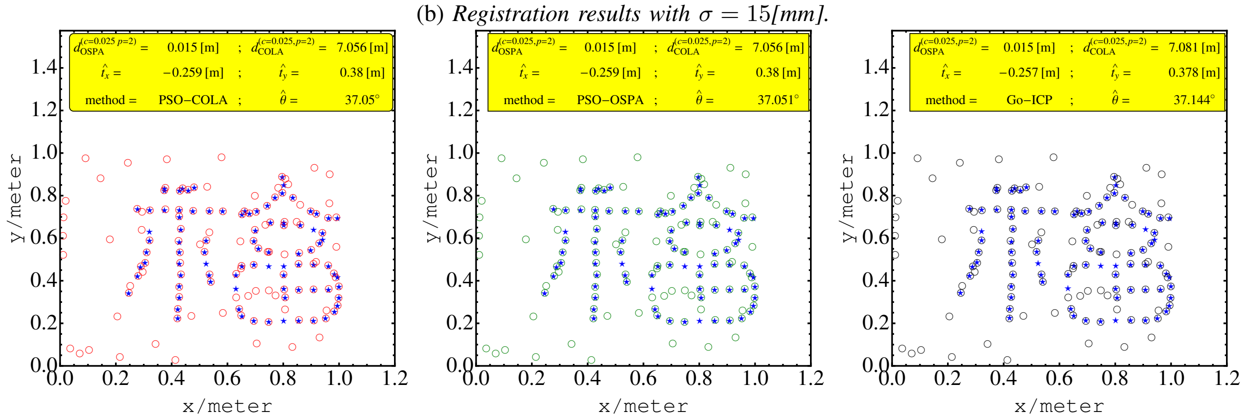

(c) *Registration results with $\sigma = 2$[mm].*

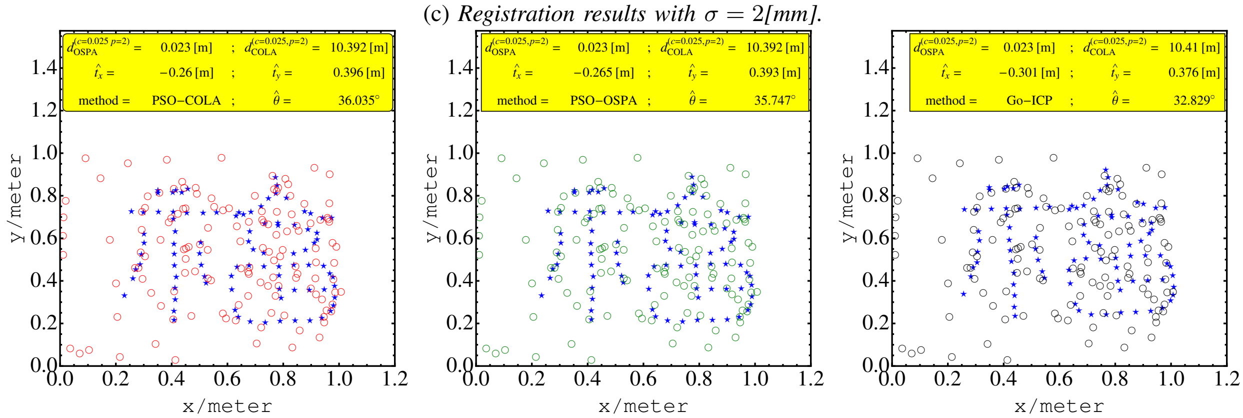

(d) *Registration results with $\sigma = 36$[mm].*

Fig. 5: *Results for the fish and Chinese character datasets of Chui & Rangarajan for various spatial errors. The blue stars represent the reference set and the red circles the model set.*

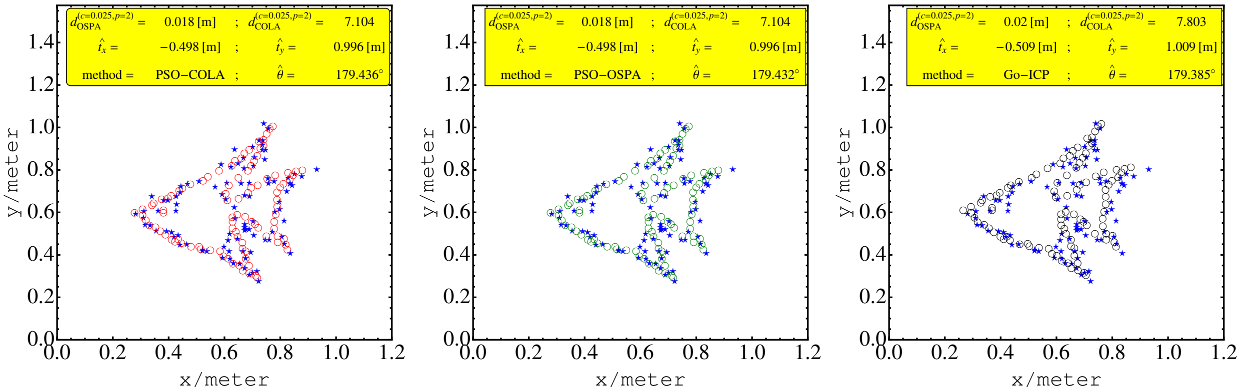

(a) *Registration results with* $E_{card} = 0$.

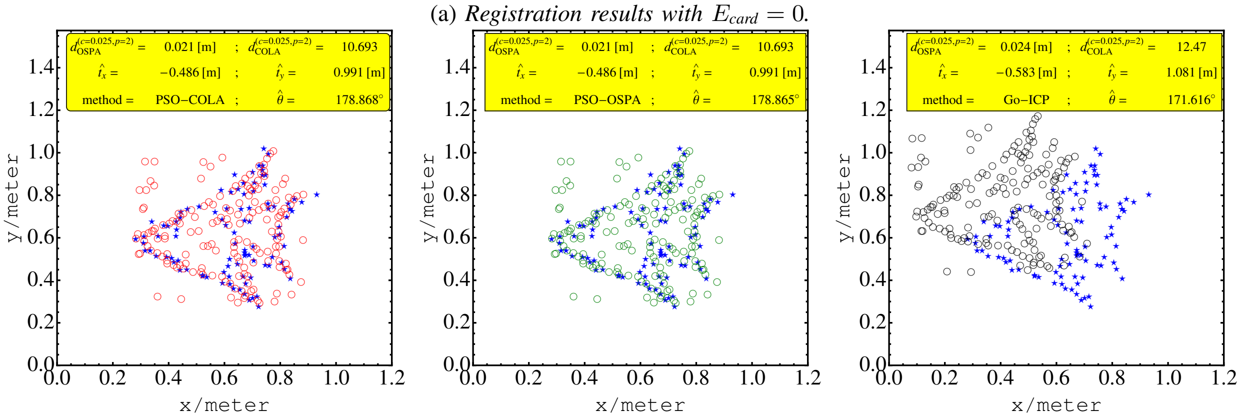

(b) *Registration results with* $E_{card} = 80$.

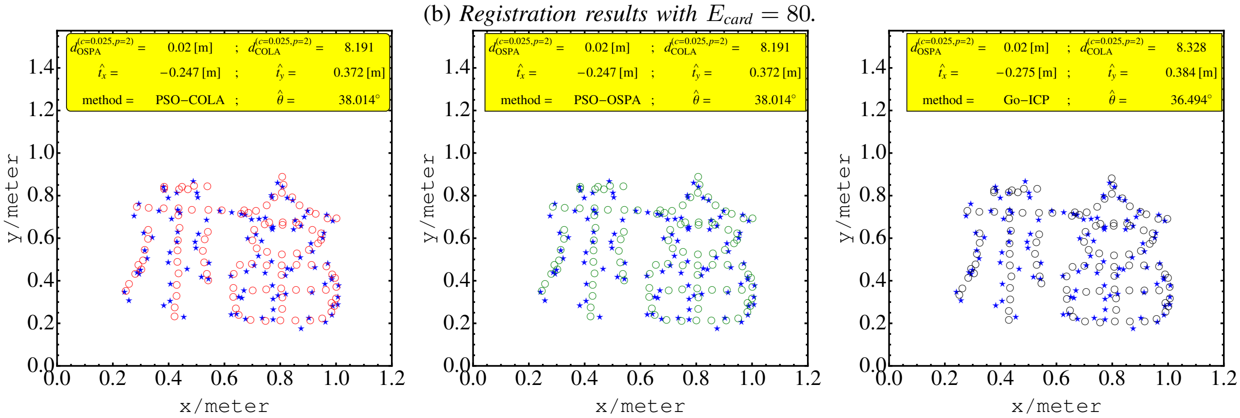

(c) *Registration results with* $E_{card} = 0$.

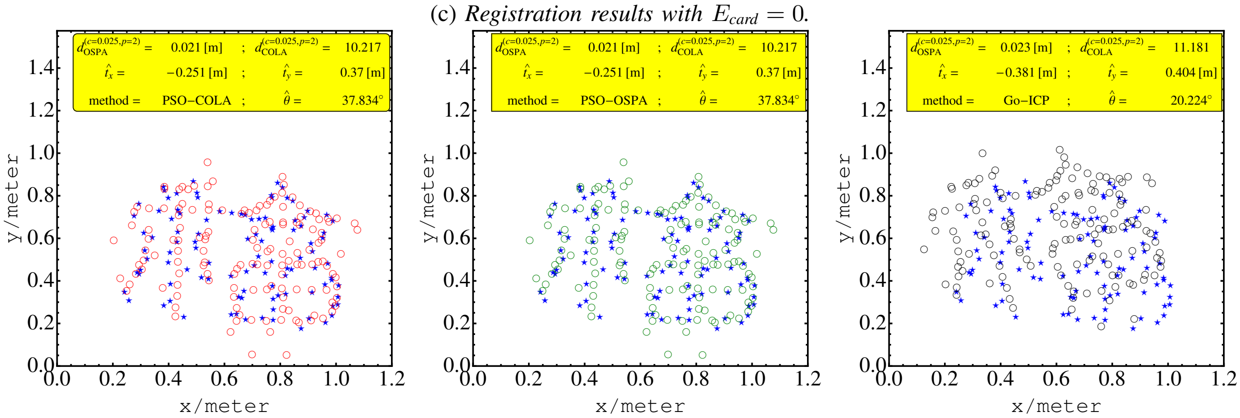

(d) *Registration results with* $E_{card} = 50$.

Fig. 6: *Results for the fish and Chinese character datasets of Chui & Rangarajan for various cardinality errors. The blue stars represent the reference set and the red circles the model set. The spatial errors have standard deviation* $\sigma = 20$*[mm].*